

# Effect of Microstructure on Fatigue Strength of Bovine Compact Bones\*

Jong Heon KIM\*\*, Mitsuo NIINOMI\*\*\*, Toshikazu AKAHORI\*\*\*,  
Junji TAKEDA\*\*\* and Hiroyuki TODA\*\*\*

Despite its clinical importance in developing artificial bone, limited information is available regarding the microstructure with respect to the fatigue characteristics of bones. In this study, the fatigue characteristics of the bovine humerus and femur were investigated with respect to microstructures. Fatigue tests were conducted on the bovine humerus and femur at a stress ratio of 0.1 and a frequency of 10 Hz. The fatigue strength of the plexiform bone is slightly greater than that of the haversian bone. This is because the volume fraction of voids in the haversian bone, which is the site of stress concentration, is higher than that of voids in the plexiform bone. Several microcracks are observed on the fatigue fracture surface of the haversian bone. The microcracks are short and their propagation directions are random. However, the number of the microcracks in the plexiform bone is very small. The microcracks are relatively long and their propagation directions are parallel to the longitudinal direction of the lamellar bone. Therefore, the crack requires relatively more energy to propagate across the lamella in the plexiform bone.

**Key Words:** Fatigue Strength, Microstructure, Microcrack, Compact Bone, Osteon

## 1. Introduction

The rapidly increasing demand for safe and high performance biomaterials for using in the elderly has led to its active research and development. There is a great demand for developing biomaterials that can be used in implant devices, such as artificial hip joints, bone plates, etc., for replacing damaged bones in the elderly. The development of artificial bone is an important issue for meeting the demand. Therefore, it is necessary to understand the mechanical properties of real bone in order to develop artificial bone.

Bone is a complex material with a multiphase, heterogeneous, and anisotropic microstructure. The processes of fracture can only be understood in terms of the underlying bone structure and its mechanical role<sup>(1)</sup>. Many researchers have investigated the mechanical properties such

as the fracture toughness, fatigue, Young's modulus and etc of bone. On the fracture toughness, Bonfield et al.<sup>(2)</sup> used the fracture mechanics method and derived the values of critical stress intensity factor ( $2.2\text{--}4.6\text{ MNm}^{-3/2}$ ) and the surface energy per unit area ( $3.9 \times 10^2\text{--}5.6 \times 10^2\text{ Jm}^{-2}$ ) in the longitudinal direction of the compact bone of bovine tibia. Using the compact tension method, Behiri et al.<sup>(3)</sup> evaluated the fracture mechanics parameters of critical stress intensity factor ( $K_c$ ) and critical strain energy release rate ( $G_c$ ) in the longitudinal direction of the compact bone in bovine tibia. They demonstrated that for a given bone density,  $K_c$  and  $G_c$  depend on the loading rate and resultant crack velocity. For a given loading rate or crack velocity, an increase in bone density resulted in increase in  $K_c$  and  $G_c$ . However, a variation in specimen thickness had no effect on the measured fracture mechanics parameters.

Particularly, research on the fatigue failure of bone is important firstly because it occurs in human beings and animals and secondly because bones are subjected to damage by cyclic loading during normal daily activities<sup>(4)–(10)</sup>. The two medical terms used to describe such failures are as follows: 1) Stress fractures, which are fatigue failures that occur due to excessive exercise; these are en-

\* Received 17th February, 2005 (No. 05-5016)

\*\* Department of Production Systems Engineering, Toyohashi University of Technology, 1-1 Hibarigaoka, Tempaku-cho, Toyohashi 441-8580, Japan.  
E-mail: kim\_93@sp-Mac4.tutse.tut.ac.jp

\*\*\* Department of Production Systems Engineering, Toyohashi University of Technology, 1-1 Hibarigaoka, Tempaku-cho, Toyohashi 441-8580, Japan

countered, for example, in athletes, soldiers, and race-horses. 2) Fragility fractures, which are fatigue failures caused by poor bone quality and is encountered in the elderly and those suffering from osteoporosis and related conditions<sup>(10),(11)</sup>. Swason et al.<sup>(12)</sup> evaluated the fatigue characteristics of fresh human femoral compact bone. In this study, the specimen surfaces were kept moist with Ringer's solution supplied from a reservoir by wick. An  $S-N$  curve was generated, and a weak correlation was observed between fatigue life and age. Carter et al.<sup>(13),(14)</sup> investigated the effects of stress amplitude, temperature, density, and microstructure on the fatigue life of bovine compact bone. Taylor et al.<sup>(15)</sup> showed that the fatigue strength of compact bone in torsion was lower than that in compression. Fergal et al.<sup>(16)</sup> introduced the concept of a microstructural barrier effect in bone, whereby cracks are initiated easily, but slow down or stop at barriers such as cement lines. In this manner, the mechanical functions of bone have been widely recognized and studied. Both trabecular and compact bone serve a mechanical function, however, the mechanism is probably specific, in part, to the type of bone. It should be clarified that the mechanical nature of bone extends beyond the simple descriptions of strength and stiffness. It also involves mechanisms by which bone avoids fatigue failure; that is, fracture due to repeated loading at the so-called physiologic load levels. However, there are few reports on the relationship between fracture characteristics and microstructure of the bone<sup>(14),(17),(18)</sup>. Therefore, in this study, the fatigue characteristics of the compact bones in bovine humerus and femur were investigated with respect to their microstructures.

## 2. Experimental Procedures

### 2.1 Materials and machining position of specimen

Cadaveric bovine humerus and femur were used as the materials in this study, as schematically shown in Fig. 1. The bones were preserved in plastic bag and stored at  $-30^{\circ}\text{C}$  prior to processing. The bovine humerus and femur were divided into anterior, posterior, medial, and lateral parts at mid-diaphyses along the bone axis direction, i.e., the longitudinal direction of the bone. Fatigue specimens were machined from the above-mentioned four parts of the bovine humerus and femur. The longitudinal direction of fatigue specimens was parallel to the longitudinal direction of the bone. The machining direction of each specimen at the mid-diaphysis of each bone is also schematically shown in Fig. 1 as a representative example.

### 2.2 Specimens

86 specimens (anterior: 13, posterior: 13, lateral: 11 and medial: 8 from the humerus and anterior: 7, posterior: 14, lateral: 10 and medial: 10 from the femur) were machined from the mid-diaphyses of 11 bovine humeri and 13 bovine femora. Smooth plate fatigue specimens

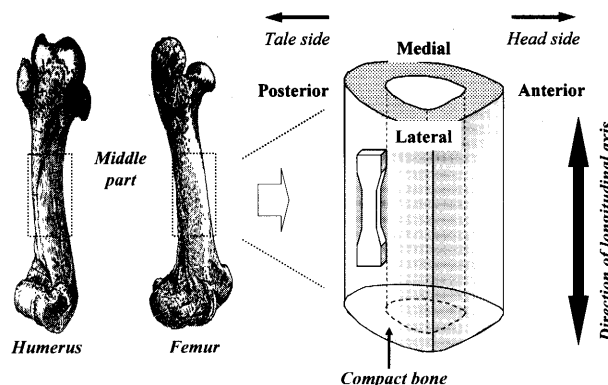


Fig. 1 Schematic drawings of bovine humerus and femur, and machining position of fatigue test specimen

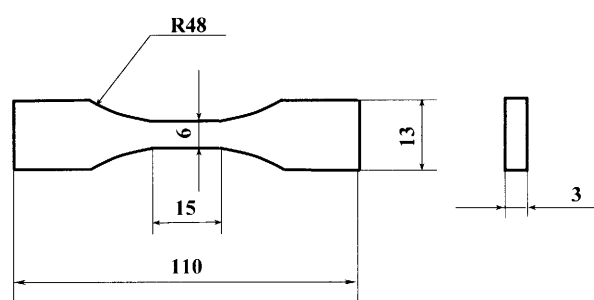


Fig. 2 Specimen geometry of fatigue test specimen in mm

with a rectangular cross-section of  $6.0\text{ mm} \times 3.0\text{ mm}$  and a gage length of 15 mm were machined according to ASTM E466-96<sup>(19)</sup> as shown in Fig. 2. The machined specimens were wet grounded using a No. 1500 waterproof emery paper. The specimens were kept moist with Ringer's solution during all the preparative steps. They were stored in Ringer's solution at  $-30^{\circ}\text{C}$  until ready for testing.

### 2.3 Fatigue test

The fatigue tests were conducted according to ASTM E446-96<sup>(19)</sup> in Ringer's solution, using an Instron machine having a capacity of 4.9 kN with a stress ratio ( $R$ ) of 0.1 and a frequency of 10 Hz. A temperature of  $36^{\circ}\text{C}$  was selected for conducting the test because it is similar to the bovine body temperature and may slightly lower the number of cycles that may be required for causing failure when compared with those required at room temperature<sup>(4)</sup>.

### 2.4 Microstructural and fracture surface observations

After the fatigue test, the one of bisected specimens was respectively cut at 5 mm and 10 mm from the fracture surface using a fine cutter. First, the former (including the fracture surface) was immersed in acetone for 30 seconds, dried slowly, coated with white gold, and examined using a scanning electron microscope (SEM). Then, the latter (fracture surface vicinity) was embedded into resin, wet grounded using a No. 1500 waterproof emery paper, and observed using a light microscope. The side surface of the vicinity of the fracture surface was observed using

a SEM. Since the microstructures of the bovine humerus and femur significantly differ according to the part, they were observed in the vicinity of fracture surface. The volume fraction of voids, haversian bone, and plexiform bone were measured in the vicinity of fracture surface. In addition, the following parameters were measured at the fracture surface of specimens of bovine humerus and femur using a SEM: the total length of microcracks, calculated by adding the lengths of all microcracks per  $\text{mm}^2$ ; the average number of microcracks per  $\text{mm}^2$ ; and the average length of microcracks, calculated by dividing the total length of microcracks by the average number of microcracks.

Using a fine cutter, the other of bisected specimens was cut at about 5 mm from the fracture surface. These portions were then embedded into resin, grounded, and observed using a light microscope. The effective crack

$$a_{\text{eff}}/a = (a_1 + a_2 + a_3 + \dots + a_n)/a$$

$a_{\text{eff}}/a$ : Effective crack propagation length  
 $a_{\text{eff}}$ : Length of crack actually propagated  
 $a$ : Crack projection length

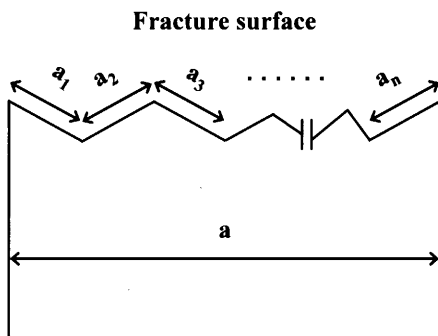


Fig. 3 Schematic drawing and equation of  $a_{\text{eff}}/a$

propagation length ( $a_{\text{eff}}/a$ ,  $a_{\text{eff}}$ : length of crack actually propagated,  $a$ : crack projection length) at the cross section of the fracture surface of the haversian and plexiform bones was measured by using the equation in Fig. 3.

### 3. Results and Discussion

The microstructure of each part of the bovine humerus and femur consists of the haversian bone, which is predominated by osteons, and the plexiform bone, which is predominated by cores of nonlamellar bone and lamellar bones in between nonlamellar bones. Figure 4 shows typical light micrographs of the haversian and plexiform bones at the mid-diaphysis. The microstructures show that the haversian bone is predominated by osteons and the plexiform bone contains cores of nonlamellar bone and blood vessels surrounded by lamellar bone present between nonlamellar bones. The microstructure of plexiform bone appears similar to a pile of thin boards.

Figure 5 shows the  $S-N$  curves of the humerus and femur. In humerus, the fatigue strength of the posterior and lateral part is greater than that of anterior and medial part. In femur, the anterior part shows the highest fatigue strength and the posterior part shows the lowest fatigue strength. Figure 6 shows the volume fractions of haversian bone, plexiform bone, and voids measured in the vicinity of fracture surface after the fatigue test. In humerus, the volume fraction of the plexiform bone is greater in the posterior and lateral parts, whereas volume fractions of haversian bone and voids are greater in anterior and medial parts. In femur, the anterior part has a high volume fraction of plexiform bone, whereas the posterior part has high volume fractions of haversian bone and voids. This indicates that fatigue strength is dependent on microstructure. The  $S-N$  curves in Fig. 7 confirm the effect of microstructure on the fatigue strength. These  $S-N$  curves were drawn using only those specimens having microstructures with

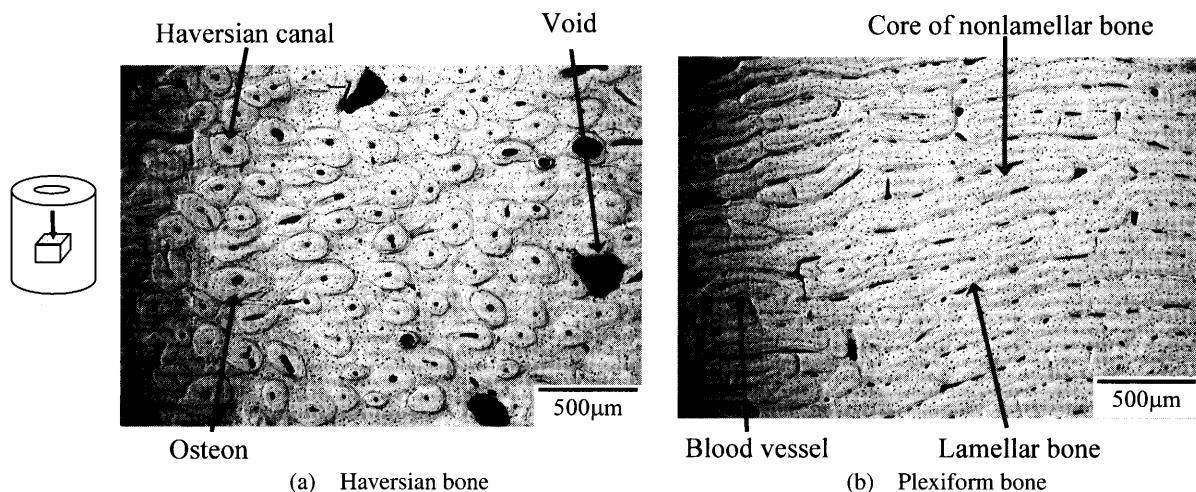


Fig. 4 Light micrographs of (a) haversian and (b) plexiform bones in mid-diaphysis of bovine femoral compact bones

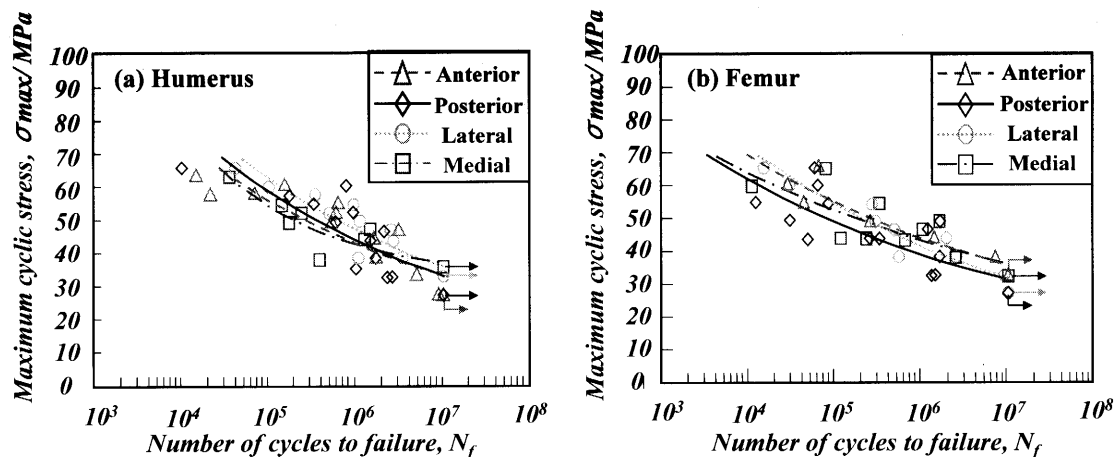


Fig. 5  $S$ - $N$  curves of various parts in mid-diaphysis of bovine (a) humeral and (b) femoral compact bones

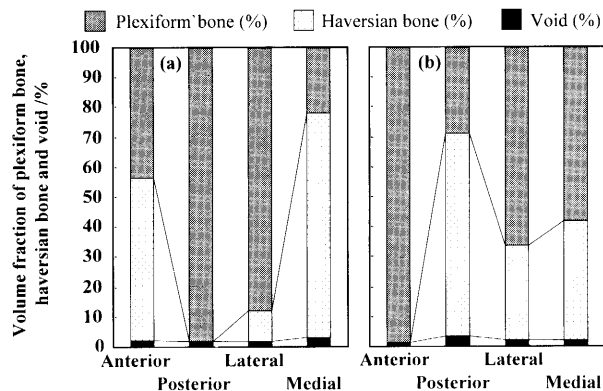


Fig. 6 Volume fractions of plexiform bone, haversian bone and voids of various parts in mid-diaphysis of bovine (a) humeral and (b) femoral compact bones

complete haversian bone or plexiform bone, confirmed in the vicinity of fracture surface of the tested specimens. In both humerus and femur, the fatigue strength of the haversian bone is lower than that of the plexiform bone. The volume fraction of voids increases with an increase in the volume fraction of haversian bone (Fig. 6). In addition, according to the report by Fleck et al.<sup>(20)</sup>, a majority of the cracks on the specimen surface initiates at the haversian and Volkmann's canals and generally end in the region of the lamellae of the osteon or interstitial bone. It has been observed that blood vessels do not stop a crack from spreading. Therefore, it is considered that the volume fraction of voids is one of the factors that exert the effect of microstructures on fatigue strength.

Figure 8 shows the fracture surface (Fig. 8(a) and (b)) and side surface in the vicinity of fracture surface (Fig. 8(c)) of haversian bone after fatigue test. Figure 8(c) shows typical main and nonpropagating cracks that initiate at the corner of the specimen. A large number of microcracks are observed on the fracture surface as shown in Fig. 8(a) and (b). The microcracks are mainly observed at

the haversian and Volkmann's canals in osteons, the interface of osteon lamellae, and voids. The failure plane of the osteons does not lie in the main fracture plane as shown in Fig. 8(a) and (b). This is because the crack grows along the osteon lamellae, and the osteons are separated from their surroundings over a certain stretch of their length<sup>(20)</sup>.

Figure 9 shows the typical fracture surface (Fig. 9(a) and (b)) and side surface in the vicinity of fracture surface (Fig. 9(c)) of plexiform bone after fatigue test. Figure 9(c) shows the typical main and nonpropagating cracks that initiate at the corner of the specimen and grow along the interface of lamellar bone, i.e., the longitudinal direction of the specimen. A large number of microcracks are observed on the fracture surface. The microcracks occur at the site of blood vessels and on the interface of lamella bones, which appears similar to a pile of thin boards. They appear like broken pieces of thread on the fracture surface of both plexiform and haversian bones. Figures 10 and 11 show typical crack propagation in the area of crack start in the plexiform and haversian bones, respectively, at the side surface of tested specimen to be observed. The nonpropagating and secondary cracks in the plexiform bone propagate longer than those in the haversian bone as shown in Figs. 8(c), 9(c), 10 and 11. This implies that the stress is more dispersed in the plexiform bone than in the haversian bone. Therefore, the second reason for fatigue strength of the plexiform bone being greater than that of the haversian bone is that the stress dispersion in the plexiform bone is greater than that in the haversian bone.

The total length, average length, and average number of microcracks per mm<sup>2</sup> observed on the fracture surface of each bone type are shown in Table 1. In addition, when the fracture surface in the plexiform bone is observed vertically, the total length of microcracks that are parallel to the longitudinal direction of lamellar bone can be measured. In femur, the total length and average number of

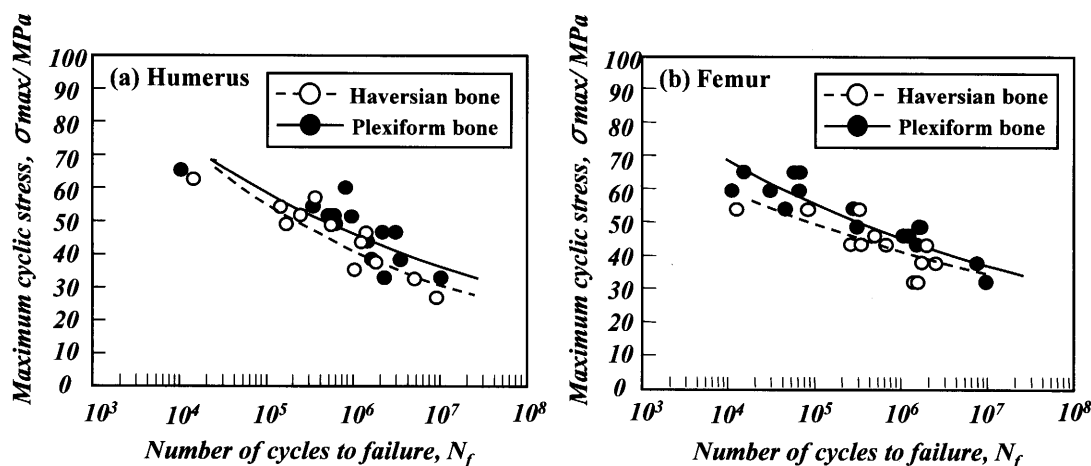


Fig. 7 *S-N* curves of haversian and plexiform bones in mid-diaphysis of bovine (a) humeral and (b) femoral compact bones

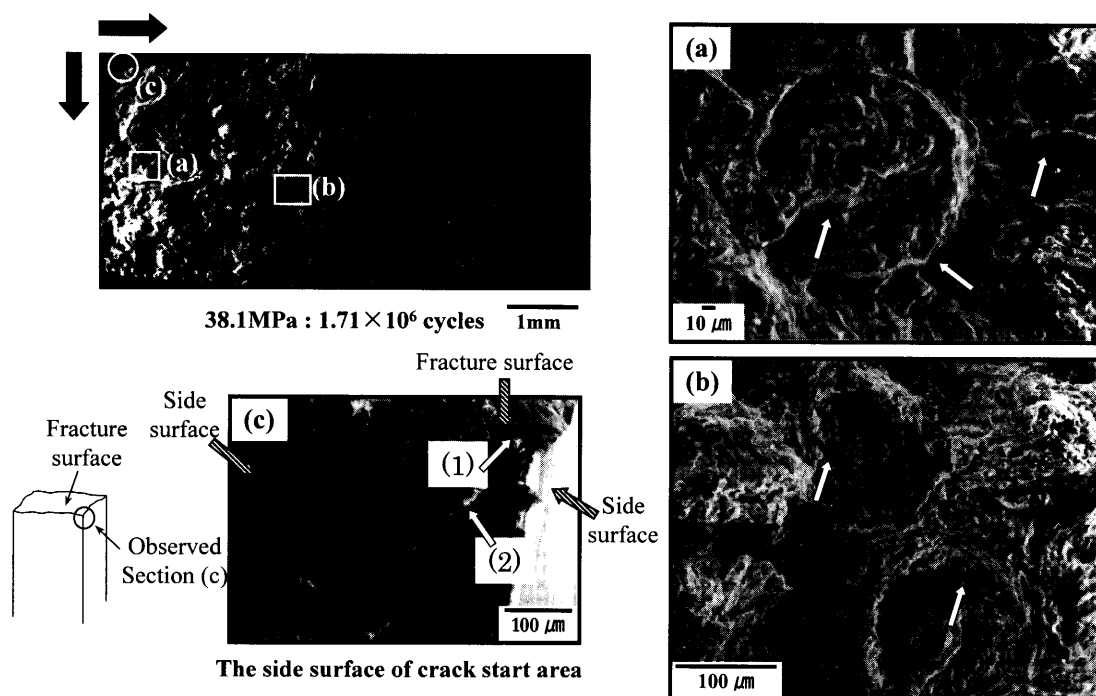


Fig. 8 SEM fractographs of haversian bone in bovine femur compact bone after fatigue test. Black arrows indicate crack propagation direction. White arrows indicate microcracks in (a) and (b) and the (1) main and (2) nonpropagating crack in (c) respectively.

microcracks are greater than those in the humerus; however, the average length of a microcrack is almost equivalent. The total length and average number of microcracks in haversian bone are greater than those in the plexiform bone, and the average length of a microcrack in haversian bone is longer in humerus than femur. In other words, the haversian bone has many short microcracks and their propagation directions are random as shown in Fig. 8 (a) and (b). This supports the findings of Norman et al.<sup>(21)</sup> who classified microcracks observed in the haversian bone into seven different categories. However, the plexiform bone has relatively fewer and long microcracks. In ad-

dition, when the fracture surface is observed vertically, 91.5% and 86.1% of the total length of microcracks in the plexiform bone of humerus and femur, respectively, are parallel to the longitudinal direction of lamella bone. This means that a majority of the microcracks propagate along the interface of lamellar bones in the plexiform bone of humerus and femur, as can be seen in Table 1 and Fig. 9 (a) and (b). Microcracks in the haversian bone are considered to easily connect to each other because their propagation directions are random. However, the microcracks, which exist among lamella bones, in the plexiform bone require greater energy to propagate across the lamel-

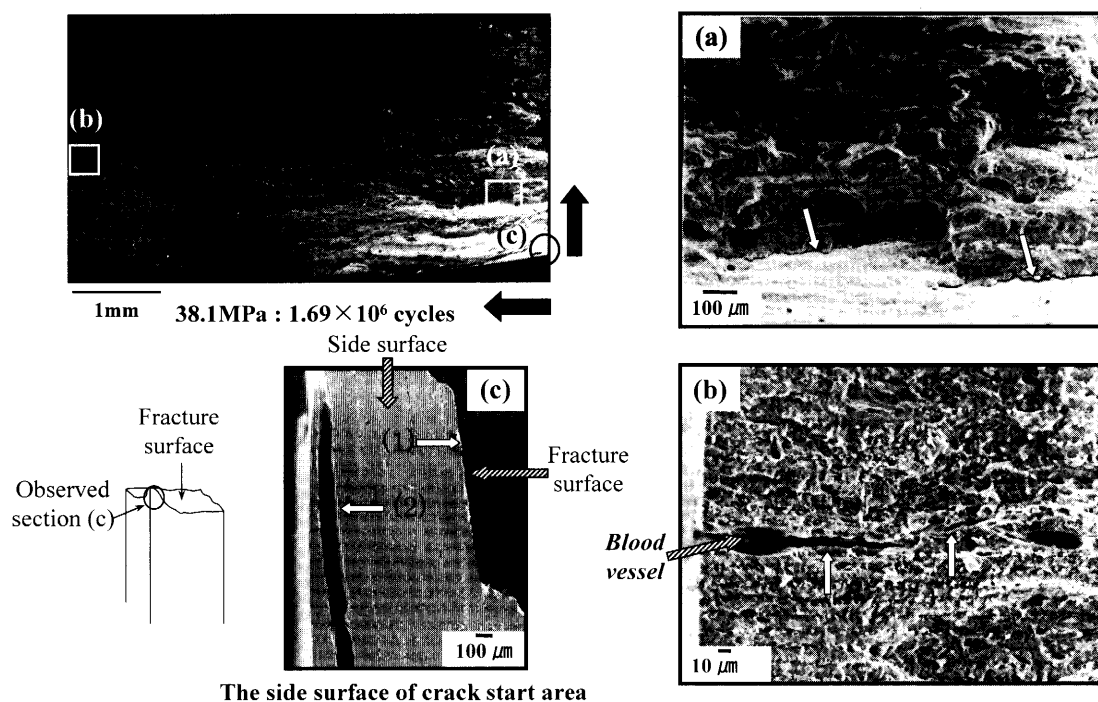


Fig. 9 SEM fractographs of plexiform bone in bovine humeral compact bone after fatigue test. Black arrows indicate crack propagation direction. White arrows indicate microcracks in (a) and (b) and the (1) main and (2) nonpropagating crack in (c) respectively.

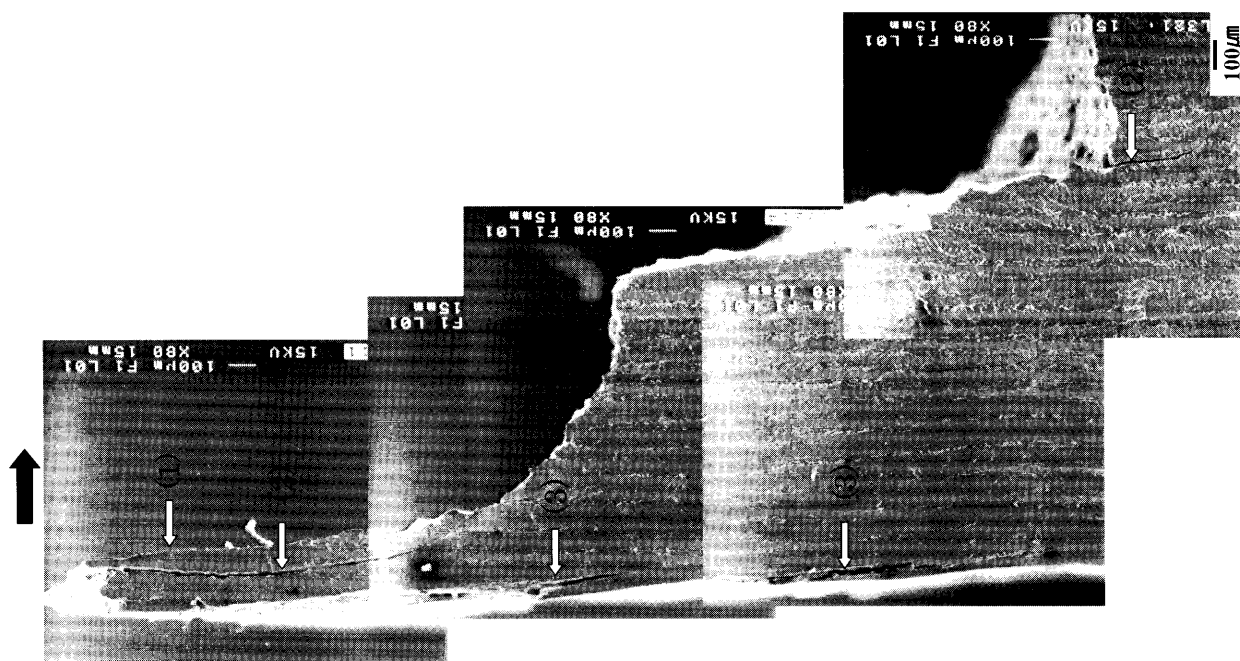


Fig. 10 SEM fractographs of the side surface of the crack start area of plexiform bone in bovine humeral compact bone after fatigue test. Black arrows indicate crack propagation direction. White arrows indicate the (1) main, (2) secondary and (3) nonpropagating crack respectively.

lar layer, although they may initiate and propagate easily at the interface of lamella bone. The lamellar layer in the plexiform bone plays a role of barrier to obstruct connecting microcracks. In other words, parallel microcracks in the plexiform bone are considered to difficulty connect to

each other because they must across lamellar layers that are existed on spaces between themselves, though they are longer than that in the haversian bone. Therefore, the third reason for fatigue strength of the plexiform bone being greater than that of the haversian bone is that the mi-

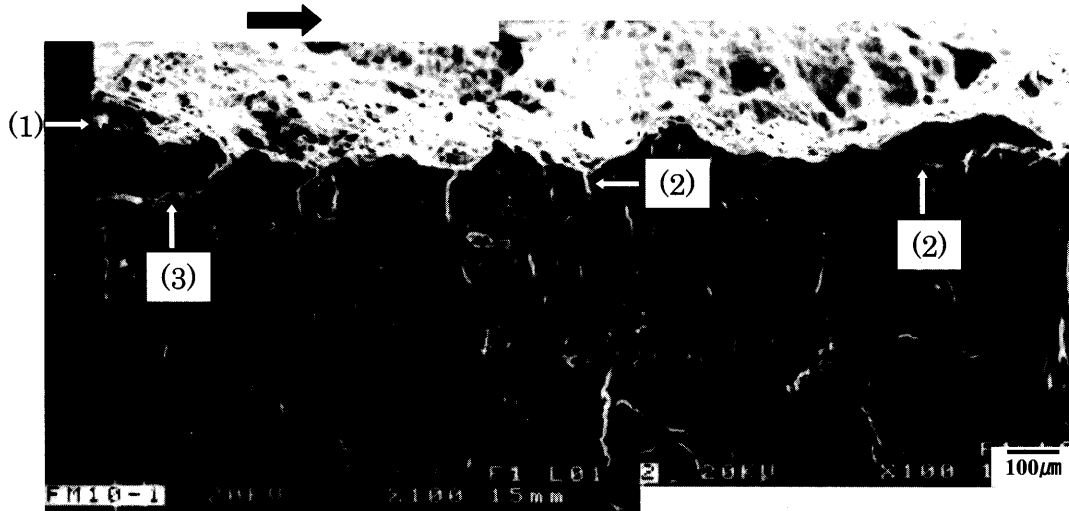


Fig. 11 SEM fractographs of the side surface of the crack start area of haversian bone in bovine humeral compact bone after fatigue test. Black arrows indicate crack propagation direction. White arrows indicate the (1) main and (2) secondary crack and (3) crack joined the main crack respectively.

Table 1 Crack length and number of microcracks observed on fracture surface of each bone type

Bone type		Total length of microcracks (mm/mm <sup>2</sup> )	Average length of microcracks (mm/mm <sup>2</sup> )	Average number of microcracks (No./mm <sup>2</sup> )	Total length of microcracks parallel to longitudinal direction of lamella bone (mm/mm <sup>2</sup> ) (%)
Humerus	Haversian bone	1.32 mm	0.149 mm	9.1	
	Plexiform bone	1.20 mm	0.220 mm	5.7	1.098 mm (91.5%)
Femur	Haversian bone	1.79 mm	0.146 mm	12.3	
	Plexiform bone	1.74 mm	0.217 mm	8.1	1.498 mm (86.1%)

crocracks of the plexiform bone require more energy to propagate across the lamella layer.

Figure 12 show  $a_{eff}/a$  of the haversian and plexiform bones. In the humerus and femur, the  $a_{eff}/a$  of the plexiform bone is greater than that of the haversian bone because the crack initiated at the corner of the specimen grew to some extent along the interface of the lamellar bone, i.e., in the longitudinal direction of the specimen for the plexiform bone, as shown in Fig. 9(c). The maximum  $a_{eff}/a$  of the plexiform and haversian bones is 1.86 and 1.35, respectively. This implies that the crack deflects more in the plexiform bone, and the crack propagation resistance is greater in the plexiform bone than in the haversian bone. Therefore, this is the fourth reason for the fatigue strength of the plexiform bone being greater than that of the haversian bone.

Figure 13 shows the schematic drawings of the crack propagation process in the haversian bone and plexiform bone. In the haversian bone, the main and nonpropagating cracks initiate at sites with high stress concentration, such as voids (haversian and Volkmann's canals) and the inter-

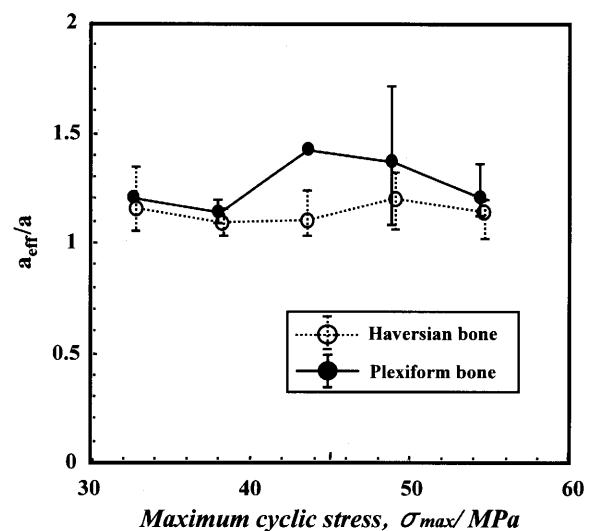


Fig. 12  $a_{eff}/a$  measured on fracture surface of haversian and plexiform bones of bovine compact bones. Each error bar shows the scatter range of data.

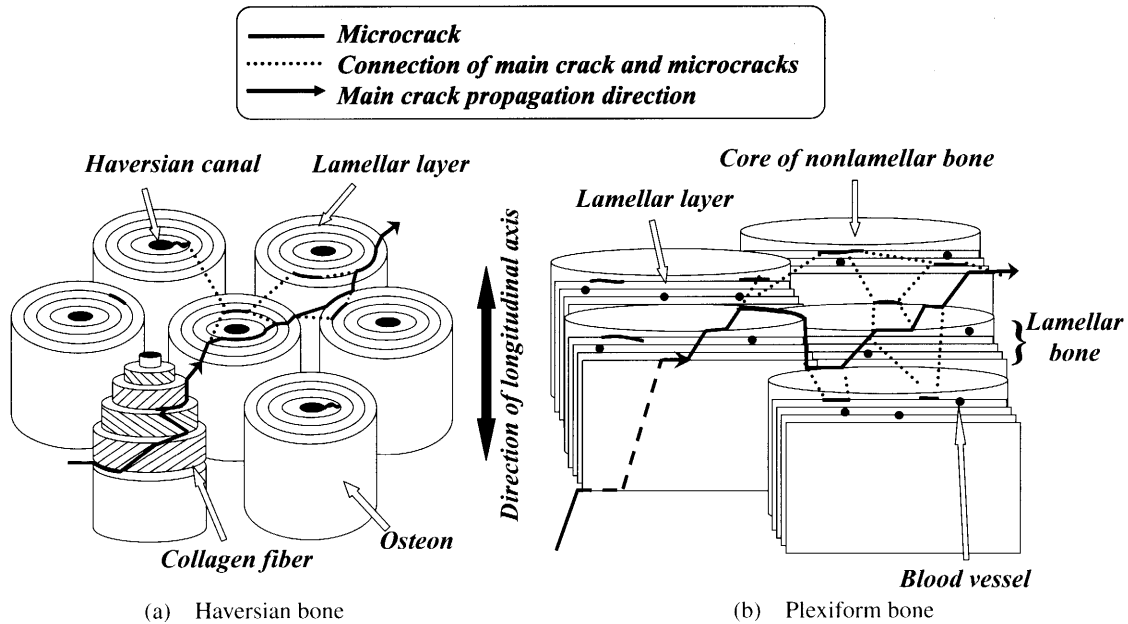


Fig. 13 Schematic drawings of crack propagation in (a) haversian and (b) plexiform bone of bovine compact bone

face of osteon lamellae on the specimen surface, propagate along these sites and then get connected with several other microcracks initiated at these sites, eventually leading to the final fracture. Similarly, in the plexiform bone, the main and nonpropagating cracks initiate at sites of high stress concentration, such as blood vessels and lamellar bone on the specimen surface, propagate along these sites, and then get connected with several other microcracks initiated at these sites, eventually leading to the final fracture.

Finally, bone is a living material and has a complex structure. Bone is a natural composite material primarily consisting of an organic phase (mostly Type 1 collagen) as matrix and a mineral phase (hydroxyapatite crystal) as reinforcement. Therefore, there are a lot of factors, such as, density, mineral content and etc. expect the microstructure, which influence a mechanical property of the bone. So that the research in this field is also important and it is a future schedule.

#### 4. Conclusions

Fatigue characteristics of bovine humerus and femur were investigated with respect to microstructures. The following results were obtained.

- (1) Fatigue strength of plexiform bones is slightly greater than that of haversian bones because the volume fraction of voids in the haversian bone is greater than that in the plexiform bone.
- (2) The stress dispersion in the plexiform bone is greater than that in the haversian bone.
- (3) According to the characteristics of the microstructure of the plexiform bone, a majority of the microcracks are parallel to the longitudinal direction of the

lamellar bone. This causes the microcrack to require relatively greater energy to propagate across the lamellar layer in the plexiform bone.

- (4) The effective crack propagation length in the plexiform bone is longer than that in the haversian bone.

(5) In haversian and plexiform bones, the main and nonpropagating cracks initiate at sites with high stress concentration, such as voids (haversian and Volkmann's canals), the interface of osteon lamellae and blood vessels, and lamellar bones on the specimen surface; propagate along these sites, and the main crack then gets connected with several microcracks initiated at these sites, eventually leading to the final fracture.

#### References

- (1) Lee, T.C., O'Brien, F.J. and Taylor, D., The Nature of Fatigue Damage in Bone, *Int. J. Fatigue*, Vol.22 (2000), pp.847–853.
- (2) Bonfield, W. and Datta, P.K., Fracture Toughness of Compact Bone, *J. Biomech.*, Vol.9 (1976), pp.131–134.
- (3) Behiri, J.C. and Bonfield, W., Fracture Mechanics of Bone—The Effects of Density, Specimen Thickness and Crack Velocity on Longitudinal Fracture, *J. Biomech.*, Vol.17 (1984), pp.25–34.
- (4) Cater, D.B., Anisotropic Analysis of Strain Rosette Information for Cortical Bone, *J. Biomech.*, Vol.10 (1978), pp.199–202.
- (5) Burr, D.B., Milgrom, C., Fyhrie, D., Forwood, M., Nyska, M., Finestone, A., Hoshaw, S., Saiag, E. and Simkin, A., In Vivo Measurement of Human Tibial Strains during Vigorous Activity, *Bone*, Vol.18 (1996), pp.405–410.
- (6) Holden, J.P. and Cavanagh, P.R., The Free Moment of



- Ground Reaction in Distance Running and Its Changes with Pronation, *J. Biomech.*, Vol.24 (1991), pp.887–897.
- (7) Martin, R.B. and Burr, D.B., A Hypothetical Mechanism for the Stimulation of Osteonal Remodeling by Fatigue Damage, *J. Biomech.*, Vol.15 (1982), pp.137–139.
  - (8) Mori, S. and Burr, D.B., Increased Intracortical Remodeling Following Fatigue Damage, *Bone*, Vol.14 (1993), pp.103–109.
  - (9) Martin, R.B., Toward a Unifying Theory of Bone Remodeling, *Bone*, Vol.26 (2000), pp.1–6.
  - (10) Doblare, M., Garcia, J.M. and Gomez, M.J., Modelling Bone Tissue Fracture and Healing, *Eng. Frac. Mech.*, Vol.71 (2004), pp.1809–1840.
  - (11) Taylor, D. and Lee, T.C., A Crack Growth Model for the Simulation of Fatigue in Bone, *Int. J. Fatigue*, Vol.25 (2003), pp.387–395.
  - (12) Swanson, S.A.V., Freeman, M.A.R. and Day, W.H., The Fatigue Properties of Human Cortical Bone, *Med. & Boil. Engng.*, Vol.9 (1971), pp.23–32.
  - (13) Carter, D.R. and Hayes, W.C., Fatigue Life of Compact Bone-I. Effects of Stress Amplitude, Temperature and Density, *J. Biomech.*, Vol.9 (1976), pp.27–34.
  - (14) Carter, D.R., Hayes, W.C. and Schurman, D.J., Fatigue Life of Compact Bone-II. Effects of Microstructure and Density, *J. Biomech.*, Vol.9 (1976), pp.211–218.
  - (15) Taylor, D., O'Reilly, P., Vallet, L. and Lee, T.C., The Fatigue Strength of Compact Bone in Torsion, *J. Biomech.*, Vol.36 (2003), pp.1103–1109.
  - (16) O'Brien, F.J., Taylor, D. and Lee, T.C., Microcrack Accumulation at Different Intervals during Fatigue Testing of Compact Bone, *J. Biomech.*, Vol.36 (2003), pp.973–980.
  - (17) Carter, D.R. and Hayes, W.C., Compact Bone Fatigue Damage-I. Residual Strength and Stiffness, *J. Biomech.*, Vol.10 (1977), pp.325–337.
  - (18) Niinomi, M., Watanabe, N., Kitaide, M., Fukui, H. and Hasegawa, J., Effect of Microstructure on Fracture Characteristics of Compact Bone, *Trans. Jpn. Soc. Mech. Eng.*, (in Japanese), Vol.64, No.168, A (1998), pp.312–318.
  - (19) ASTM E466-96, Standard Practice for Conducting Force Controlled Constant Amplitude Axial Fatigue Tests of Metallic Materials, (1997), pp.480–484.
  - (20) Fleck, C. and Eifler, D., Deformation Behavior and Damage Accumulation of Cortical Bone Specimens from the Equine Tibia under Cyclic Loading, *J. Biomech.*, Vol.36 (2003), pp.179–189.
  - (21) Norman, T.L. and Wang, Z., Microdamage of Human Cortical Bone: Incidence and Morphology in Long Bones, *Bone*, Vol.20 (1997), pp.375–379.